

# FUNDUS AUTOFLUORESCENCE PATTERNS IN CENTRAL SEROUS CHORIORETINOPATHY

JISANG HAN, MD,\* NAM SUK CHO, MD,† KIYOUNG KIM, MD,‡ EUNG SUK KIM, MD, PhD,‡ DO GYUN KIM, MD, PhD,§ JOON MO KIM, MD, PhD,\* SEUNG-YOUNG YU, MD, PhD‡

**Purpose:** To investigate the patterns of fundus autofluorescence (FAF) abnormalities in patients with central serous chorioretinopathy (CSC).

**Methods:** This cross-sectional observational study included 126 eyes of 118 patients who were diagnosed with central serous chorioretinopathy from December 2006 to April 2012 at Kyung Hee University Hospital, Seoul, Korea. Fundus autofluorescence patterns were analyzed with spectral domain optical coherence tomography and visual acuity.

**Results:** Fundus autofluorescence patterns were grouped as blocked (38.9%), mottled (8.7%), hyper (31.0%), hyper/hypo (13.5%), or descending tract (8.0%). The duration of symptoms was 7.8 ( $\pm 20.4$ ), 28.3 ( $\pm 31.8$ ), 42.5 ( $\pm 69.1$ ), 163.8 ( $\pm 183.5$ ), and 174.5 ( $\pm 162.3$ ) days in the blocked, mottled, hyper, descending tract, and hyper/hypo groups, respectively ( $P < 0.001$ ). The blocked FAF group had the best visual acuity ( $P = 0.011$ ). The intact ellipsoid zone on the spectral domain optical coherence tomography was mostly found in the blocked FAF group ( $P < 0.001$ ), and the disrupted ellipsoid zone was commonly exhibited in the hyper/hypo and descending tract groups. Disrupted external limiting membrane line on the spectral domain optical coherence tomography was seen in two patients of the descending tract group only.

**Conclusion:** The FAF abnormalities in central serous chorioretinopathy show multiple patterns and are related with the chronicity and visual acuity. Fundus autofluorescence patterns in central serous chorioretinopathy are helpful when considering the timing of treatment and predicting the disease status.

RETINA 40:1387–1394, 2020

Central serous chorioretinopathy (CSC) is an idiopathic syndrome occurring in young to middle-aged adults, characterized by serous detachment of the neu-

rosensory retina. It is also associated with leakage of fluid from the choroid and focal leakage at the level of the retinal pigment epithelium (RPE).<sup>1–9</sup> In the early phases of the acute CSC, the visual acuity is relatively good despite the presence of serous retinal detachment. Later, patients often complain of blurred vision, micropsia, and metamorphopsia. The acute form of this disease generally resolves spontaneously, with a return to almost normal visual acuity.<sup>10–12</sup> However, the chronic form of this disease is often associated with visual acuity decline and atrophic and degenerative changes of the retina and RPE.<sup>6</sup> However, there are no definitive criteria to distinguish between acute and chronic CSC, as the criteria remain unclear. The current classification of such patients depends on the symptom duration that they recall.<sup>4,13,14</sup> Singh et al<sup>15</sup> reported the high discordance among retina specialists in describing CSC subtypes and demonstrated the need for a refined classification system of CSC.

From the \*Department of Ophthalmology, Kangbuk Samsung Hospital, Sungkyunkwan University School of Medicine, Seoul, Republic of Korea; †Jeil Eye Clinic, Suwon, Republic of Korea; ‡Department of Ophthalmology, Kyung Hee University Hospital, Seoul, Republic of Korea; and §Department of Ophthalmology, Myongji Hospital, Hanyang University Medical Center, Seoul, Republic of Korea.

Presented as an instructional course at the annual meeting of the American Academy of Ophthalmology, Chicago, IL, November 12, 2012.

None of the authors has any financial/conflicting interests to disclose.

This is an open-access article distributed under the terms of the Creative Commons Attribution-Non Commercial-No Derivatives License 4.0 (CCBY-NC-ND), where it is permissible to download and share the work provided it is properly cited. The work cannot be changed in any way or used commercially without permission from the journal.

Reprint requests: Seung-Young Yu, MD, PhD, Department of Ophthalmology, Kyung Hee University Hospital, 23 Kyungheedaero, Dongdaemun-gu, Seoul 02447, Republic of Korea; e-mail: syyu@khu.ac.kr

Fundus autofluorescence (FAF) is a noninvasive method that provides functional images of the fundus, by using the stimulated emission of light from endogenous fluorophores, the most significant being lipofuscin. Lipofuscin is generated as a by-product of the retinoid cycle after the phagocytosis of photoreceptor outer segments (OS) by the RPE and demonstrates fluorescence between 500 nm and 750 nm with a peak emission at 630 nm.<sup>16</sup> Hyperautofluorescence in CSC arises from the RPE or the accumulated photoreceptor outer segment not being phagocytized by the RPE or macrophages with a phagocytized outer segment.<sup>17</sup> Excessive accumulation of lipofuscin represents a common pathogenetic pathway in various monogenetic and complex retinal diseases and is believed to precede photoreceptor degeneration.<sup>18–20</sup> Fundus autofluorescence detects changes of fluorophores, reflects the status of the RPE activity, and reveals changes in the retina over the early and late CSC. Thus, recently, FAF imaging has been widely used to study CSC.<sup>2,5,13,21–40</sup> Morphological retinal changes in the outer retinal layer also lead to abnormal FAF owing to the abnormal retinol metabolism and lipofuscin accumulation.<sup>41</sup> By analyzing the association between FAF, chronicity, visual acuity, and spectral domain optical coherence tomography (SD-OCT) in a large sample size, we can infer the association between FAF pattern and CSC status. In addition, when determining whether to hold or start active treatment, FAF patterns would be helpful in distinguishing acute from chronic CSC. In this study, we analyzed the FAF patterns of CSCs, classifying them into five groups. Each FAF pattern was then analyzed based on the visual acuity, the accompanying SD-OCT findings, and the symptom duration.

## Methods

### *Patients*

This study involved a retrospective review of the medical records of consecutive patients with idiopathic CSC, who were examined at the Kyung Hee University Hospital, Seoul, Korea, from December 2006 to April 2012. This study was approved by the Institutional Review Board Committee of Kyung Hee University Hospital. This research adhered to the tenets of the Declaration of Helsinki. All patients diagnosed with idiopathic CSC during the period were analyzed. The idiopathic CSC was diagnosed when serous detachment of the neurosensory retina, including the macula, was confirmed by SD-OCT, leakage at the RPE level was shown in fluorescein angiography (FA), and choroidal hyperpermeability was noted in

indocyanine green angiography (ICGA). The subjects included were those with symptoms for CSC involving the macular area. Patients with neovascular maculopathy such as age-related macular degeneration, polypoidal choroidal vasculopathy, idiopathic choroidal neovascularization, or retinal vascular diseases were excluded from the study. Patients with intraocular inflammation, optic disk pit, or posterior segmental tumor were excluded. Patients who had undergone laser photocoagulation or photodynamic therapy for CSC were excluded from the study. Eyes with bilateral involvement were analyzed individually.

All patients underwent a complete ophthalmologic examination including best-corrected visual acuity (BCVA), slit-lamp biomicroscopy, fundus photography, FA, ICGA, SD-OCT, and FAF imaging. Best-corrected visual acuity was measured with the standard Snellen chart at 6 m and converted into the logarithm of the minimum angle of resolution visual acuity for statistical analysis.

A confocal scanning laser ophthalmoscope (cSLO, Heidelberg Retina Angiograph 2 system; Heidelberg Engineering, Heidelberg, Germany), combined with SD-OCT (SPECTRALIS HRA + OCT; Heidelberg Engineering) was used to acquire simultaneous imaging of the retinal morphology and FAF. Retinal fluorescence was excited by 488-nm pulsed blue laser light and detected with a barrier filter at 500 nm.

An abnormal FAF was defined as either an increased or decreased FAF signal when compared with the normal background FAF, outside of such lesions.<sup>35</sup> We classified FAF imaging into five patterns as blocked AF, mottled AF, hyper AF, hyper/hypo AF, or descending tract. A pattern was defined as blocked FAF if there were no changes or uniform changes in decreased autofluorescence where subretinal fluids (SRFs) existed (Figure 1); mottled FAF showed a grainy or coarse region of increased FAF when compared with the normal surrounding background fluorescence (Figure 2); hyper FAF showed an increased FAF signal when compared with that outside the lesion (referred to as normal FAF) (Figure 3); hyper/hypo FAF was characterized by a mixed form of hyperautofluorescence and hypoautofluorescence (Figure 4); and descending tract exhibited a downward leading swathe of decreased autofluorescence originating from the posterior pole to extend below the level of the inferior arcade (Figure 5).<sup>27</sup> To assess the interobserver variability for this novel FAF classification, two independent retinal specialists, E.S.K. and S.-Y.Y., classified FAF images along the predominant FAF pattern at the posterior pole. The analysis was repeated after 1 week to determine intraobserver variability.

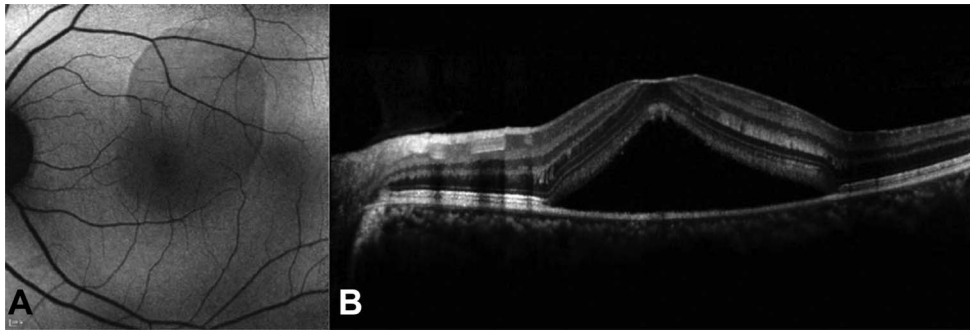


**Fig. 1.** Fundus autofluorescence image (A) shows a homogeneous background fluorescence and a uniform change from the FAF of the normal background (blocked FAF). There is a decrease in the FAF intensity where the SRF existed and shows uniform changes. Spectral domain optical coherence tomography image (B) shows SRF in the region where the FAF intensity decreased.

The status of the foveal external limiting membrane (ELM) and the ellipsoid zone (EZ) on the SD-OCT images was judged to be either intact or disrupted. The protruding mass at the OS line in the area of serous retinal detachment was described as OS elongation. When there are focal hyperreflective protruding masses at the RPE layer and in the space between the RPE layer and the Bruch membrane, it is defined as an RPE proliferation.

#### Statistical Analyses

Statistical analysis was performed using the PASW statistics tool (version 18.0.0, SPSS Inc., Chicago, IL). We investigated the correlation between the FAF patterns, BCVA, and the SD-OCT findings, using the Kruskal–Wallis and Fisher's exact test. Intra-observer and interobserver variability was determined with  $\kappa$  statistics. For all tests,  $P$  value  $< 0.05$  was defined as statistically significant.

### Results

The subjects of this study were 126 eyes of 118 patients. The mean patient age was 46.5 ( $\pm 9.2$ ) years, with 100 men (84.7%) and 18 women (15.3%). The mean logarithm of the minimum angle of resolution

BCVA was 0.32 ( $\pm 0.32$ ) (20/40). Eight patients (6.8%) showed bilateral CSC (Table 1).

The eyes were classified into five different patterns according to the results of topographic alteration in FAF. They were classified as blocked FAF (49 eyes, 38.9%), mottled FAF (11 eyes, 8.7%), hyper FAF (39 eyes; 30.0%), hyper/hypo FAF (17 eyes, 13.5%), and descending tract (10 eyes, 7.9%). Classification of the FAF images, by 2 independent observers, resulted in an agreement in 82.5% of the cases. The interobserver variability was  $\kappa = 0.76$  (95% confidence interval, 0.77–0.93). The intraobserver variability for observer I was  $\kappa = 0.86$  (95% confidence interval, 0.72–0.89) and for observer II was  $\kappa = 0.82$  (95% confidence interval, 0.66–0.85).

There was a difference in the duration of symptoms according to the FAF patterns. The blocked FAF ( $7.8 \pm 20.4$  days) showed the shortest duration of symptoms, followed by the mottled FAF ( $28.3 \pm 31.8$  days), hyper FAF ( $42.5 \pm 69.1$  days), hyper/hypo FAF ( $174.5 \pm 162.3$  days), and descending tract ( $163.8 \pm 183.5$  days) ( $P < 0.001$ ). Best-corrected visual acuity also showed that the blocked FAF had a better acuity ( $P = 0.011$ , Table 2). The intact EZ of the SD-OCT images seemed to be more pronounced with the blocked, mottled, and hyper FAF than hyper/hypo FAF and descending tract ( $P < 0.001$ , Table 2). Markedly, all eyes of the blocked FAF showed intact EZ. The

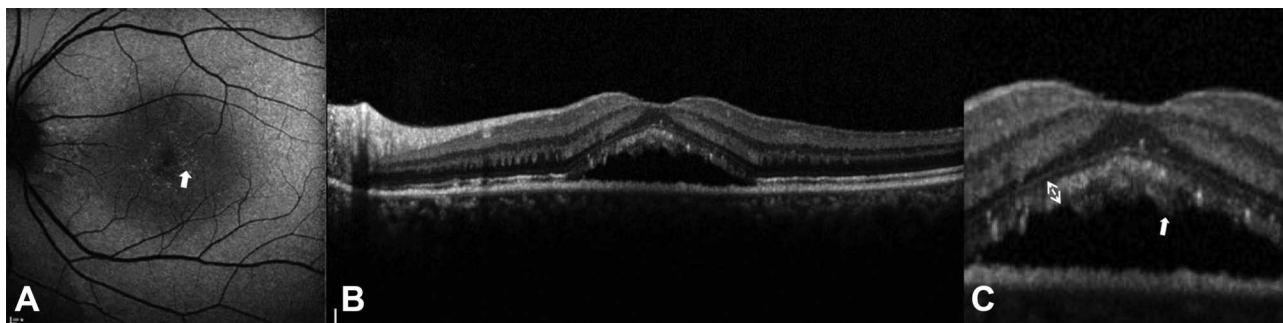
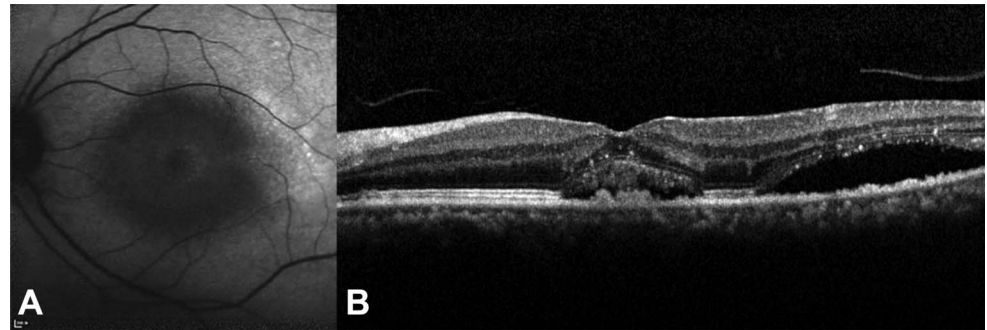


**Fig. 2.** Fundus autofluorescence image (A) shows a grainy or coarse region (white arrow) of increased FAF compared with the FAF of normal background (mottled FAF). Spectral domain optical coherence tomography image (B) shows SRF. Spectral domain optical coherence tomography image of the foveal and parafoveal regions (C) shows outer segment elongation (dotted double arrow) and subretinal deposits (white arrow).

**Fig. 3.** Fundus autofluorescence image (A) shows an increase in FAF intensity around the macula and in the temporal area, compared with the FAF of normal background (hyper FAF). Spectral domain optical coherence tomography image (B) shows an elongation of the photoreceptor's outer segments around the macula and loss of photoreceptor of the temporal area that results in increased transmission of retinal pigment epithelium fluorescence.



disrupted ELM was found only in 2 cases of the descending tract group ( $P = 0.006$ ; Figure 5 and Table 2). OS elongation was frequently found in the mottled FAF, the hyper FAF, and the hyper/hypo FAF ( $P < 0.001$ ; Figure 2 and Table 2). There was also a difference in the RPE proliferation according to FAF patterns ( $P < 0.001$ ), and it was frequently found in the hyper FAF, the hyper/hypo FAF, and the descending tract groups (Figure 3 and Table 2).

### Discussion

Fundus autofluorescence imaging is an imaging method that allows topographic mapping of lipofuscin distribution in the RPE as well as of other fluorophores that may occur with the disease of the outer retina and the subneurosensory retinal space.<sup>42</sup> In this study, we have classified patterns of FAF into the blocked FAF, the mottled FAF, the hyper FAF, the hyper/hypo FAF, or the descending tract in the eyes with CSC.

The blocked FAF pattern was characterized by no change in autofluorescence or by a uniformly decreased autofluorescence. The decreased autofluorescence is most likely to be related to the blockage of the FAF signal by the SRF.<sup>43</sup> Blocked FAF is believed to be present in the early phase of the disease, considering

the short duration of symptoms as seen in our results. The mottled FAF pattern showed diffusely speckled hyperautofluorescence. We confirmed that this pattern is likely related to the longer duration of SRF when compared with the blocked FAF. This may result from the patchy accumulation of the shed photoreceptor OS that is autofluorescent due to the fluid shifting into the lobulated subretinal space over time.<sup>17,42,44,45</sup> Matsumoto et al<sup>30</sup> reported that the increased mottled FAF seemed to originate from the elongated photoreceptor OS, in the detached retina. With time, patchy accumulation in the subretinal space distributed generally and uniformly within the subretinal space, i.e., increased diffused FAF was demonstrated. Symptom duration was longer in patients with hyper FAF when compared with the mottled FAF. As time passed, the hypo FAF was demonstrated in damaged RPE due to the mechanical damages by SRF and the accumulated autofluorescent materials. It was proposed that as hypo FAF occurred in the hyper FAF area, hyper FAF and hypo FAF coexist.<sup>49</sup> In addition, chronic patients had varying degrees of atrophy including broader areas of geographic atrophy in the macula and gravity-driven fluid tracks descending inferiorly. These tracts were typically hyperautofluorescent when the fluid first occurred but became increasingly hypoautofluorescent as the RPE cells got damaged in the pathway of the fluid

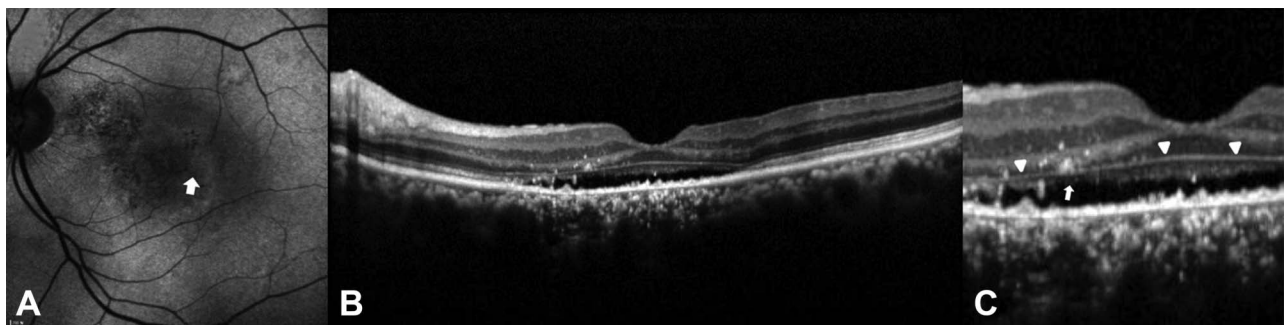


**Fig. 4.** Fundus autofluorescence image (A) with hyperautofluorescence and hypoautofluorescence (hyper/hypo FAF). Spectral domain optical coherence tomography images (B) and (C) show intact ELM (pointing triangles) and disruption of the EZ (white arrow).

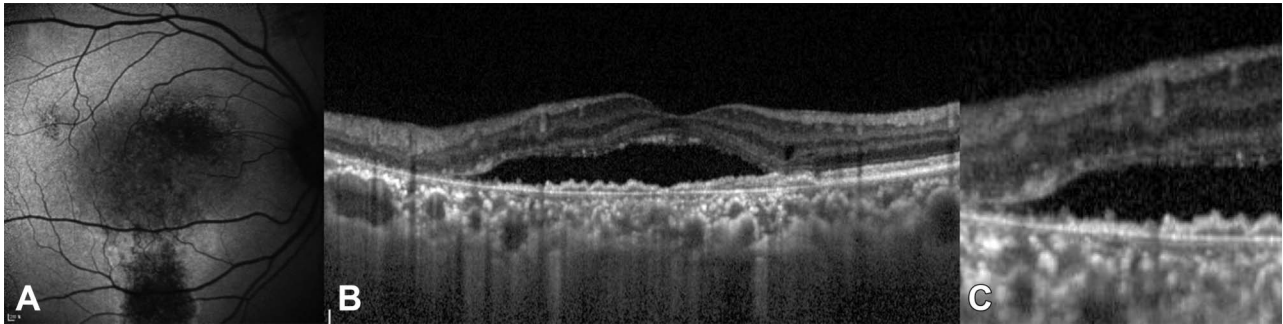


**Fig. 5.** Fundus autofluorescence image (A) shows a downward leading swathe of decreased autofluorescence, originating from the posterior pole and extending below the level of the inferior arcade (descending tract). Spectral domain optical coherence tomography images (B) and (C) show the disruption of the ELM and the EZ.

(Figure 6).<sup>1</sup> In this study, this was termed the descending tract group.

Lee et al<sup>5</sup> reported FAF patterns in CSC according to the course of the disease. They analyzed the FAF findings by dividing the patients with CSC into acute, chronic, and sequela. They observed hyper FAF, hypo FAF, or minimal changes at acute CSC and discrete hyper FAF dots or descending tract at chronic CSC. They reported that these FAF findings helped with the more accurate assessment of the disease status and prognosis and helped with the proper treatment modality used in the clinic. Our findings support these arguments. We performed more detailed classification in our study. We classified FAF images first without information about the chronicity and analyzed visual acuity and symptom duration of patients in each group. In a study conducted by Lee et al,<sup>5</sup> many of the findings of acute CSC and chronic CSC were found in patients in our study, and their chronicity was also consistent with our study.

Zola et al<sup>46</sup> reported FAF pattern changes over time in patients with chronic CSC. The most common baseline pattern in their study was granular hypo FAF. Subsequently, the earliest change in chronic CSC was a diffuse hyper FAF followed by the development of hypo FAF spots with time. These FAF pattern changes are similar to our findings. However, Zola et al reported that this change in FAF is very slow and not good for use in clinical trials. The FAF pattern changes in our study occurred very slowly, as reported by Zola et al, and the degree of change and time varied from person to person, making it difficult for it to be used in a clinical trial. However, since we can deduce the status of the disease, we think that the FAF pattern can help us decide whether it is time to consider active treatment.

Dysli et al<sup>2</sup> demonstrated shorter fluorescence lifetimes in acute CSC and prolonged fluorescence lifetimes in chronic CSC due to increased concentrations of lipofuscin. They showed that FAF change was

associated with worse visual acuity. They also reported that fluorescence lifetimes may give a clue to the functional state of the photoreceptors as short lifetimes may suggest that the phototransduction cycle is still intact while the appearance of longer lifetimes may suggest structural damage. Our findings that visual acuity was poor in groups with large changes in FAF are consistent with their report, although there are differences in the study methodology.

In our study, the blocked FAF showed the best visual acuity among all others. This suggests that the visual acuity could be maintained with intact ELM and EZ because the serous retinal detachment duration is shorter and less perturbed due to the closed SRF. The hyper/hypo and descending tract groups showed the least favorable visual prognosis in our study. Similar results were reported by Imamura et al<sup>27</sup> where confluent and granular hypofluorescence and descending tract were related to decreased vision. This result may be derived from disrupted EZ due to chronicity. Some of the interesting findings of this study were that the frequency of disrupted EZ increased in FAF patterns with longer duration of symptoms and that decreased visual acuity corresponded to disrupted EZ. Ojima et al<sup>4</sup> reported similar results where the eyes with defects at the subfoveal inner segment/outer

Table 1. Clinical Characteristics of Patients

Variables	Data
No. of eyes	126
No. of patients	118
Mean age (yrs)	46.5 ± 9.2
Sex, N (%)	
Men	100 (84.7)
Women	18 (15.3)
Mean BCVA LogMAR (Snellen equivalent)	0.32 ± 0.32 (20/40)
Mean duration of symptom (weeks)	55.2 ± 106.6

LogMAR, logarithm of the minimum angle of resolution.

Table 2. Difference in Patient Characteristics Among Fundus Autofluorescence Patterns

	Blocked AF	Mottled AF	Hyper AF	Hyper/ Hypo AF	Descending Tract	P
Number	49	11	39	17	10	
Duration of symptom (days)	7.8 ± 20.4	28.3 ± 31.8	42.5 ± 69.1	174.5 ± 162.3	163.8 ± 183.5	<0.001*
Mean BCVA LogMAR (Snellen equivalent)	0.21 ± 0.26 (20/32)	0.36 ± 0.31 (20/40)	0.35 ± 0.34 (20/40)	0.48 ± 0.38 (20/50)	0.47 ± 0.32 (20/50)	0.011*
Disruption of EZ junction, N (%)	0 (0)	1 (9.1)	2 (5.1)	9 (52.9)	7 (70.0)	<0.001†
Disruption of ELM, N (%)	0 (0)	0 (0)	0 (0)	0 (0)	2 (20.0)	0.006†
OS elongation, N (%)	3 (6.1)	6 (54.5)	29 (74.4)	7 (41.2)	0 (0)	<0.001†

LogMAR, logarithm of the minimum angle of resolution; OS, photoreceptor outer segments.

\*Kruskal–Wallis test.

†Fisher’s exact test.

segment (IS/OS) junction had poor visual acuity. Thus, FAF patterns could be used to predict disease chronicity and visual prognosis. OS elongation was found frequently in the mottled FAF, hyper FAF, and hyper/hypo FAF groups, but not in the descending tract group ( $P = 0.082$ ). This is in agreement with other reports that both OS and IS were elongated during the development of the disease and outer plexiform layer thinning occurred with time.<sup>14,47</sup>

Yu et al<sup>48</sup> divided the OCT finding of the outer border of the photoreceptor in CSC into smooth, granulated, and scattered dots attached to the ELM. The median symptom duration of each finding was 18, 180, and 1,855 days respectively. These findings are similar to those seen in our study. In our study, the findings of the outer segment elongation and subretinal deposits (Figures 2 and 3) in the mottled the FAF, hyper FAF, and hyper/hypo FAF groups corresponded to the “granulated” group in their study. The disruption of the EZ seen in the descending tract FAF group in our study corresponded to the “scattered dot” group in their study, and the trend of symptom duration is also similar.

Retinal pigment epithelium proliferation was found in the descending tract, hyper/hypo FAF, hyper FAF, mottled FAF, and blocked FAF groups, in the order of

frequency, which was in accordance with the duration of symptoms. Retinal pigment epithelium proliferation may be due to sustained pressure on pigment epithelial detachment over time. This mechanical RPE defect may be compensated with RPE cellular proliferation.<sup>24</sup>

The agreement of the FAF classification was 82.5%, and the k-values of intraobserver and interobserver variability were between 0.76 and 0.86 in our study; this was equivalent to the FAF classification of age-related macular degeneration, with an agreement of 82% and k-values from 0.74 to 0.8.<sup>43</sup> This reveals the reliability of the FAF classification system in our study.

When evaluating CSC, an understanding of the chronicity of the disease is important for determining the treatment plan. Generally, CSC is divided into acute or chronic according to a duration period of 3 months or 6 months. However, there has been no objective standard to evaluate the chronicity of CSC. Our study demonstrated the correlation between visual acuity and FAF pattern, in relation with the duration of symptoms, and showed that FAF imaging could be used to predict the chronicity of CSC.

The limitation to this study includes its retrospective design and the small number of patients in each FAF pattern group. Another limitation to this study is that

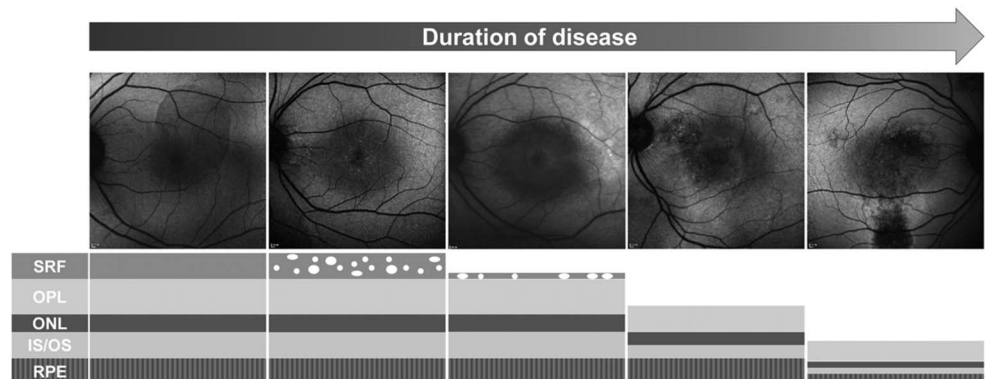


Fig. 6. Diagram showing the changes of fluorescence and microstructure of the outer retina and the RPE of patients with CSC. ONL, outer nuclear layer; OPL, outer plexiform layer.

the duration of symptoms is dependent on the subjective recall of the patient, so there may be some disagreement regarding its exact duration. However, objective determination of symptom duration is not possible. Therefore, this is an inborn error.

In conclusion, FAF imaging may be used as a supplementary diagnostic tool to evaluate the chronicity of CSC and help determine the treatment plan. Also, the current study showed that the FAF patterns corresponded to the integrity of EZ and correlated with chronicity and visual acuity, which may be associated with the chronicity of the disease. Further investigations on FAF patterns and CSC in larger patient groups will allow us to identify the disease characteristics of each patient by analyzing FAF patterns, including responses to treatment, and prognosis.

**Key words:** autofluorescence, central serous chorioretinopathy, classification, optical coherence tomography.

### References

- Nicholson B, Noble J, Forooghian F, Meyerle C. Central serous chorioretinopathy: update on pathophysiology and treatment. *Surv Ophthalmol* 2013;58:103–126.
- Dysli C, Berger L, Wolf S, Zinkernagel MS. Fundus autofluorescence lifetimes and central serous chorioretinopathy. *Retina (Philadelphia, Pa)* 2017;37:2151–2161.
- Gass JD. Pathogenesis of disciform detachment of the neuroepithelium. *Am J Ophthalmol* 1967;63:1–139.
- Ojima Y, Hangai M, Sasahara M, et al. Three-dimensional imaging of the foveal photoreceptor layer in central serous chorioretinopathy using high-speed optical coherence tomography. *Ophthalmology* 2007;114:2197–2207.
- Lee WJ, Lee JH, Lee BR. Fundus autofluorescence imaging patterns in central serous chorioretinopathy according to chronicity. *Eye (Lond)* 2016;30:1336–1342.
- Spaide RF, Campeas L, Haas A, et al. Central serous chorioretinopathy in younger and older adults. *Ophthalmology* 1996; 103:2070–2079; discussion 2079–2080.
- Aggio FB, Roisman L, Melo GB, et al. Clinical factors related to visual outcome in central serous chorioretinopathy. *Retina* 2010;30:1128–1134.
- Chen SN, Hwang JF, Tseng LF, Lin CJ. Subthreshold diode micropulse photocoagulation for the treatment of chronic central serous chorioretinopathy with juxtafoveal leakage. *Ophthalmology* 2008;115:2229–2234.
- Wang M, Munch IC, Hasler PW, et al. Central serous chorioretinopathy. *Acta Ophthalmol* 2008;86:126–145.
- Fok AC, Chan PP, Lam DS, Lai TY. Risk factors for recurrence of serous macular detachment in untreated patients with central serous chorioretinopathy. *Ophthalmic Res* 2011;46:160–163.
- Ficker L, Vafidis G, While A, Leaver P. Long-term follow-up of a prospective trial of argon laser photocoagulation in the treatment of central serous retinopathy. *Br J Ophthalmol* 1988; 72:829–834.
- Liegl R, Ulbig MW. Central serous chorioretinopathy. *Ophthalmologica* 2014;232:65–76.
- Framme C, Walter A, Gabler B, et al. Fundus autofluorescence in acute and chronic-recurrent central serous chorioretinopathy. *Acta Ophthalmol Scand* 2005;83:161–167.
- Fujimoto H, Gomi F, Wakabayashi T, et al. Morphologic changes in acute central serous chorioretinopathy evaluated by fourier-domain optical coherence tomography. *Ophthalmology* 2008;115:1494–1500.
- Singh SR, Matet A, van Dijk EHC, et al. Discrepancy in current central serous chorioretinopathy classification. *Br J Ophthalmol* 2018. [Epub ahead of print]
- Weinberger AW, Lappas A, Kirschkamp T, et al. Fundus near infrared fluorescence correlates with fundus near infrared reflectance. *Invest Ophthalmol Vis Sci* 2006;47:3098–3108.
- Spaide RF, Klancnik JM Jr. Fundus autofluorescence and central serous chorioretinopathy. *Ophthalmology* 2005;112: 825–833.
- Wing GL, Blanchard GC, Weiter JJ. The topography and age relationship of lipofuscin concentration in the retinal pigment epithelium. *Invest Ophthalmol Vis Sci* 1978;17:601–607.
- Dorey CK, Wu G, Ebenstein D, et al. Cell loss in the aging retina. Relationship to lipofuscin accumulation and macular degeneration. *Invest Ophthalmol Vis Sci* 1989;30:1691–1699.
- Weiter JJ, Delori FC, Wing GL, Fitch KA. Retinal pigment epithelial lipofuscin and melanin and choroidal melanin in human eyes. *Invest Ophthalmol Vis Sci* 1986;27:145–152.
- Ayata A, Tatlipinar S, Kar T, et al. Near-infrared and short-wavelength autofluorescence imaging in central serous chorioretinopathy. *Br J Ophthalmol* 2009;93:79–82.
- Choi KE, Yun C, Kim YH, et al. The effect of photopigment bleaching on fundus autofluorescence in acute central serous chorioretinopathy. *Retina* 2017;37:568–577.
- Dinc UA, Tatlipinar S, Yenerel M, et al. Fundus autofluorescence in acute and chronic central serous chorioretinopathy. *Clin Exp Optom* 2011;94:452–457.
- Eandi CM, Ober M, Iranmanesh R, et al. Acute central serous chorioretinopathy and fundus autofluorescence. *Retina (Philadelphia, Pa)* 2005;25:989–993.
- Eandi CM, Piccolino FC, Alovise C, et al. Correlation between fundus autofluorescence and central visual function in chronic central serous chorioretinopathy. *Am J Ophthalmol* 2015;159: 652–658.
- Ho IV, Yannuzzi L. Chronic central serous chorioretinopathy and fundus autofluorescence. *Retin Cases Brief Rep* 2008;2:1–5.
- Imamura Y, Fujiwara T, Spaide RF. Fundus autofluorescence and visual acuity in central serous chorioretinopathy. *Ophthalmology* 2011;118:700–705.
- Kim SK, Kim SW, Oh J, Huh K. Near-infrared and short-wavelength autofluorescence in resolved central serous chorioretinopathy: association with outer retinal layer abnormalities. *Am J Ophthalmol* 2013;156:157–164.e152.
- Lindner E, Weinberger A, Kirschkamp T, et al. Near-infrared autofluorescence and indocyanine green angiography in central serous chorioretinopathy. *Ophthalmologica* 2012;227:34–38.
- Matsumoto H, Kishi S, Sato T, Mukai R. Fundus autofluorescence of elongated photoreceptor outer segments in central serous chorioretinopathy. *Am J Ophthalmol* 2011;151:617–623.e611.
- Nam KT, Yun CM, Kim JT, et al. Central serous chorioretinopathy fundus autofluorescence comparison with two different confocal scanning laser ophthalmoscopes. *Graefes Arch Clin Exp Ophthalmol* 2015;253:2121–2127.
- Oh J, Kim SW, Kwon SS, et al. Correlation of fundus autofluorescence gray values with vision and microperimetry in

- resolved central serous chorioretinopathy. *Invest Ophthalmol Vis Sci* 2012;53:179–184.
33. Ozmert E, Batioğlu F. Fundus autofluorescence before and after photodynamic therapy for chronic central serous chorioretinopathy. *Ophthalmologica* 2009;223:263–268.
  34. Pang CE, Shah VP, Sarraf D, Freund KB. Ultra-widefield imaging with autofluorescence and indocyanine green angiography in central serous chorioretinopathy. *Am J Ophthalmol* 2014;158:362–371.e362.
  35. Roisman L, Lavinsky D, Magalhaes F, et al. Fundus autofluorescence and spectral domain OCT in central serous chorioretinopathy. *J Ophthalmol* 2011;2011:706849.
  36. Sekiryu T, Iida T, Maruko I, et al. Infrared fundus autofluorescence and central serous chorioretinopathy. *Invest Ophthalmol Vis Sci* 2010;51:4956–4962.
  37. Shin JY, Choi HJ, Lee J, et al. Fundus autofluorescence findings in central serous chorioretinopathy using two different confocal scanning laser ophthalmoscopes: correlation with functional and structural status. *Graefes Arch Clin Exp Ophthalmol* 2016;254:1537–1544.
  38. Teke MY, Elgin U, Nalcacioglu-Yuksekkaya P, et al. Comparison of autofluorescence and optical coherence tomography findings in acute and chronic central serous chorioretinopathy. *Int J Ophthalmol* 2014;7:350–354.
  39. Zhang P, Wang HY, Zhang ZF, et al. Fundus autofluorescence in central serous chorioretinopathy: association with spectral-domain optical coherence tomography and fluorescein angiography. *Int J Ophthalmol* 2015;8:1003–1007.
  40. von Rückmann A, Fitzke FW, Fan J, et al. Abnormalities of fundus autofluorescence in central serous retinopathy. *Am J Ophthalmol* 2002;133:780–786.
  41. Iacono P, Battaglia PM, Papayannis A, et al. Acute central serous chorioretinopathy: a correlation study between fundus autofluorescence and spectral-domain OCT. *Graefes Arch Clin Exp Ophthalmol* 2015;253:1889–1897.
  42. Schmitz-Valckenberg S, Holz FG, Bird AC, Spaide RF. Fundus autofluorescence imaging: review and perspectives. *Retina* 2008;28:385–409.
  43. Bindewald A, Bird AC, Dandekar SS, et al. Classification of fundus autofluorescence patterns in early age-related macular disease. *Invest Ophthalmol Vis Sci* 2005;46:3309–3314.
  44. Liu J, Itagaki Y, Ben-Shabat S, et al. The biosynthesis of A2E, a fluorophore of aging retina, involves the formation of the precursor, A2-PE, in the photoreceptor outer segment membrane. *J Biol Chem* 2000;275:29354–29360.
  45. Fishkin N, Jang YP, Itagaki Y, et al. A2-rhodopsin: a new fluorophore isolated from photoreceptor outer segments. *Org Biomol Chem* 2003;1:1101–1105.
  46. Zola M, Chatziralli I, Menon D, et al. Evolution of fundus autofluorescence patterns over time in patients with chronic central serous chorioretinopathy. *Acta Ophthalmol* 2018;96:e835–e839.
  47. Song IS, Shin YU, Lee BR. Time-periodic characteristics in the morphology of idiopathic central serous chorioretinopathy evaluated by volume scan using spectral-domain optical coherence tomography. *Am J Ophthalmol* 2012;154:366–375.e364.
  48. Yu J, Jiang C, Xu G. Correlations between changes in photoreceptor layer and other clinical characteristics in central serous chorioretinopathy. *Retina (Philadelphia, Pa)* 2018. [Epub ahead of print]
  49. Nicholson B, Noble J, Forooghian F, Meyerle C. Central serous chorioretinopathy: update on pathophysiology and treatment. *Surv Ophthalmol* 2013;58:103–126.